International Journal of Civil Engineering (2021) 19:549–561
https://doi.org/10.1007/s40999-020-00574-9

RESEARCH PAPER

Effect of Silt Content on Liquefaction Susceptibility of Fine Saturated River Bed Sands

Pradipta Chakrabortty[1] · Nishant Nilay[1] · Angshuman Das[1]

Received: 21 April 2020 / Revised: 15 September 2020 / Accepted: 24 September 2020 / Published online: 12 October 2020

Abstract

The effect of silt intrusion on the liquefaction susceptibility of fine saturated sand has been studied here using a series of strain-controlled cyclic triaxial tests on isotropically consolidated soil specimens. The fine sands used in this study were collected from the Ganga and Sone river bed. The samples were prepared with 100% non-plastic silt, 100% sand and different percentage (5%, 10%, 20%, and 30%) of non-plastic silt mixed with fine sand to study the effect of intruded silt on liquefaction susceptibility of sand. It has been found that at the same relative density range (10–25%) and the same percentage of intruded non-plastic silt, the Ganga sand is having higher liquefaction susceptibility than the Sone sand. The outcome of the study also showed that the rate of generation of excess pore water pressure (EPWP) for all three soil specimens was more or less same at higher strain levels (0.66–1.31%). However, the liquefaction potential continues to increase with the increase in silt content at a lower strain rate of 0.13%. A graphical relationship has been proposed for the EPWP development model parameter as a function of non-plastic silt content. This modification in the EPWP model parameter is one of the novel aspects presented here, which can be used for site-specific nonlinear ground response analysis.

Keywords Liquefaction · Fine sand · Non-plastic silt · Strain-controlled test · Cyclic triaxial

Abbreviations

C_c	Coefficient of curvature
C_u	Coefficient of uniformity
D_{10}	Effective size of particles corresponding to 10% finer in the particle size distribution curve
D_{30}	Diameter of particles corresponding to 30% finer in the particle size distribution curve
D_{50}	Mean grain diameter
D_{60}	Diameter of particles corresponding to 60% finer in the particle size distribution curve
p, F and s	*EPWP* Model parameter
ε	Cyclic axial strain
γ_c	Cyclic shear strain
σ'_h	Effective stress acting on the horizontal direction
σ'_m	Mean principal effective stress
σ'_v	Effective stress acting on soil on the vertical direction

✉ Pradipta Chakrabortty
pradipt@iitp.ac.in

Nishant Nilay
nishantnilay.iitp@gmail.com

Angshuman Das
angshuman.pce15@iitp.ac.in

[1] Department of Civil and Environmental Engineering, IIT Patna, Patna 801106, India

1 Introduction

Liquefaction is an undesirable phenomenon that occurs due to substantial or total loss of shear strength and stiffness of soil during a cyclic or monotonic loading. The loss of shear strength and stiffness of soil may cause because of reduction in effective stress of soil deposit under cyclic loading condition. The liquefaction is dependent on various parameters that vary from one place to another like relative density, soil type, water table depth, and topography, etc. It has generally been observed that loose saturated cohesionless soil deposits are highly susceptible to liquefaction; however, the presence of fines in the sand has always shown a muddling behaviour under seismic loading condition. The soil can be classified as "sand-like" and "clay-

like" soil based on its cyclic behaviour [1, 2]. The 'sand-like' soils are gravels, sands, and low plastic silts, whereas 'clay-like' soils are clays and plastic silts. The 'sand-like' soils can experience liquefaction, and its behaviour has become the area of research for the last few decades. The clay-like soils can also experience cyclic failure and significant ground deformation during an earthquake [3, 4].

Case studies from previous earthquakes (e.g., Haicheng in 1975; Tangshan in 1976) indicate that soil having clay content less than 20% had liquefied. Moreover, the field investigation after the Tokachioki earthquake by [5] showed that the presence of a higher proportion of plastic fines increased the liquefaction resistance [6] of sand layers. Therefore, the main focus of this study was to quantify the effect of non-plastic silts intruded in the sand in terms of cyclic behaviour under cyclic loading condition. In the last couple of decades, the impact of non-plastic fines in the sand has been studied by various researchers [7–12]. A summary of significant literature to quantify the effect of fines content (*FC*) on liquefaction resistance (*LR*) using cyclic triaxial tests are tabulated in Table 1 [9, 11, 13–23, 35, 47].

There are many factors such as sample preparation technique, confining pressure, loading frequency, global void ratio, intergranular void ratio and type of test (stress- or strain-controlled) that control the outcomes. It can be observed from the literature that no conclusive remark can be drawn from the previous studies on cyclic/monotonic load response of sand-silt mixture. Therefore, due to divergence outcomes of previous studies, the cyclic response of sand impinged by the silt of different percentages (0%, 5%, 10%, 20%, 30% and 100%) by weight under cyclic loading condition has been studied in this research. The main objective was to inspect the cyclic behaviour of locally available sands, i.e. Sone and Ganga sand at different silt content. It has been done through strain-controlled undrained cyclic triaxial tests. A part of the study on Ganga sand mixed with non-plastic silt has already been presented by [15]. A comparison between the cyclic response of Sone and Ganga sand intruded by silt based on mean grain diameter ratio ($D_{50\ sand}/D_{50\ silt}$) has been presented at $\pm$ 0.5 mm axial displacement amplitude.

Further investigation has been carried out to find out the effect of the applied cyclic strain level. The results show that at higher strain levels (0.66–1.31%) the rate of generation of excess pore water pressure (EPWP) for all three soil specimens are more or less same. Liquefaction strength of a soil depends on the amount and rate of EPWP development and can be estimated using a strain-based mathematical model proposed by [24]. This model calculates the EPWP ratio as a function of the number of loading cycles. The EPWP model parameters (F is one of them) in this model depend on grain size, saturation condition, and void ratio, as documented in the literature [25, 26]. Another novel aspect studied here is the effect of non-plastic silt content on EPWP model parameter F. A graphical relation has been presented for EPWP model parameter F with the percentage of the silt present in the sand matrix.

2 Material Used

The soil used in this study is locally available sand collected from the alluvial deposit. The geology of the region is greatly influenced by the fine sands deposited by Sone and Ganga river [27]. Particle size distribution and specific gravity confirming to IS: 2720 (part-4) [28] and IS: 2720 (part-3) [29] respectively have been carried out. As shown in Fig. 1, the Sone and Ganga river sand get classified into poorly graded, and the silt particle that is being used is having the smallest size of around 10 μm. The other important characteristics related to particle size distribution have been tabulated in Table 2. The specific gravity for all the soil samples was found to be lying in between 2.67 and 2.72. The maximum and minimum dry density of soil is not unique as it is very much dependent on the method used for its determination [30]. The maximum dry densities for all the soil samples were measured using heavy compaction test confirming to IS: 2720 (part-8) [31]. Dry density obtained using heavy compaction yielded little bit higher values than that obtained using the vibratory table. For the minimum dry density of soil samples, ASTM D 4254-16 [32] method C has been used in this study. Using the relationship between dry density and void ratio, maximum and minimum void ratio of all soil (Sone and Ganga sand intruded with various percentages of silt) samples were obtained and is shown in Fig. 2. Consistency limit of silt confirming to IS: 2720 (part-5) [33] was obtained, and the test results suggest that the liquid limit value for the silt that is being used is less than 2%. Furthermore, it was observed that molding the sample into a thread of 3.2 mm was not possible because of very low plasticity. Hence, it has been ascertained that the silt used in the study is non-plastic. Silt used in this study is collected from the top layer of IIT Patna soil. Since the particle size of Ganga sand was smaller than Sone sand hence the presence of space for accommodating silt particles would also be lesser than the Sone sand matrix. The X-ray diffraction (XRD) patterns of various soils obtained from the XRD analysis are shown in Fig. 3. From the XRD analysis, it has been observed that minerals such as quartz, calcite, smectite and plagioclase are present in Ganga sand. Apart from these above mentioned minerals, actinolite is also present in non-plastic silt and Sone sand.

Table 1 Summary of significant literature showing the requirement of the present study

Comparison basis	Test type	Fines content (FC)	$\frac{D_{50,sand}}{D_{50,silt}}$	Effect on liquefaction resistance	References
Constant void ratio	Cyclic triaxial	0–60%	–	Increases	[16]
Constant void ratio	Stress controlled cyclic triaxial	0–20%	20.83	Increases	[35]
Constant sand skeleton void ratio					
Constant void ratio	Strain controlled cyclic triaxial	0–100%	35.29	Decrease up to a limiting value of silt content which is 30% silt content	[47]
Constant relative density	Cyclic triaxial	0–60%	–	Decreases till 20% FC then increases	[17]
Constant void ratio	Stress controlled cyclic triaxial	10–50%	–	Increases	[18]
Constant void ratio	Stress controlled cyclic triaxial	0–100%	14.33	Decreases till 35% FC then increases	[19]
Constant sand skeleton void ratio				Constant till limiting fine content (LFC)	
Constant relative density			6	Constant till limiting silt content then decrease	
Constant sand skeleton void ratio				Increases till limiting silt content	
Constant void ratio	Stress controlled cyclic triaxial	0–100%	6	Decreases till LFC then increases	[9]
Constant void ratio	Strain controlled cyclic direct shear	0–10%	41.67	Increases	[20]
Constant sand skeleton void ratio		0–20%		Increases till 10% FC and then decreases	
Constant relative density		0–20%		Increases till 10% FC when γ = 0.03% and maximum at 20% FC when γ = 0.3%	
Constant gross void ratio	Stress controlled cyclic triaxial	0–60%	10.1	Decreases till LFC (approx. varies between 20 and 30% depending on the post-consolidation void ratio) then increases	[21]
Constant sand skeleton void ratio		0–60%		Remain same till the silt content corresponding to D_r = 70% then increases	
Constant relative density		0–100%		Initially increases till 5%, decreases till LFC (30%) then remain constant	
Constant relative density	Stress controlled cyclic triaxial	0–40%	10.52	Decreases	[22]
Constant relative density	Strain controlled monotonic triaxial	0–20%	2.6 5.9 10.1	For same FC and confining pressure, LR increases with decrease in $D_{50\ Sand}/D_{50\ Silt}$ ratio	[23]
Constant relative density	Strain controlled cyclic triaxial	0–20%	11.67	Increases till the optimum value of silt content (approx. 15% silt content)	[13]
Constant dry density	Stress controlled cyclic triaxial	0–100%	9.23	Decreases till LFC (about 30% silt content) then increases	[11]
Constant relative density				Decreases till LFC (about 30% silt content) then constant	

Table 1 (continued)

Comparison basis	Test type	Fines content (FC)	$\frac{D_{50,sand}}{D_{50,silt}}$	Effect on liquefaction resistance	References
Constant void ratio	Static triaxial	0–100%	9.2	Decreased till LFC (approx. 30% silt content) then increases	[14]
Constant relative density				Decreased till LFC (approx. 30% silt content) then constant	
Constant relative density	Strain controlled cyclic triaxial	0–100%	4.4	Increased till 10% then decreased	[16]

3 Experimental Scheme

The cyclic response of Sone and Ganga sand intruded with the different percentages by weight of non-plastic silt has been studied here using the strain-controlled cyclic triaxial test. A series of 18 strain-controlled cyclic triaxial tests were performed at the soil dynamics lab of IIT Patna using the hydraulic controlled cyclic triaxial testing equipment (shown in Fig. 4). These tests were conducted with various combinations of silt percentage mixed with natural Sone or Ganga river sand (details of these experiments are shown in Table 3). All tests were performed in undrained conditions on isotropically consolidated specimens, as per the guidelines provided in ASTM D-5311 [34].

3.1 Specimen Preparation

There are several methods for soil specimen preparation, e.g., dry air pluviation, dry and moist tamping and wet tamping etc. According to [35], a higher degree of uniformity can be observed in soil specimen prepared using dry deposition technique, while moist tamping method yields considerable non-uniformity. The steady-state line

Table 2 Properties of the Sone and Ganga sand used in the study

Grain size range	Sone sand 2 mm–75 μm	Ganga sand 2 mm–75 μm	Silt 75–2 μm
$D_{50,\ sand}$	0.3	0.2	0.045
$D_{50,\ sand}/D_{50,\ silt}$	6.67	4.44	–
D_{60}	0.33	0.23	0.05
D_{30}	0.23	0.18	0.03
D_{10}	0.18	0.16	–
C_u	1.83	1.44	–
C_c	0.89	0.88	–
Liquid limit/plastic limit	–	–	< 2/non-plastic
Classification	Poorly graded	Poorly graded	Non-plastic

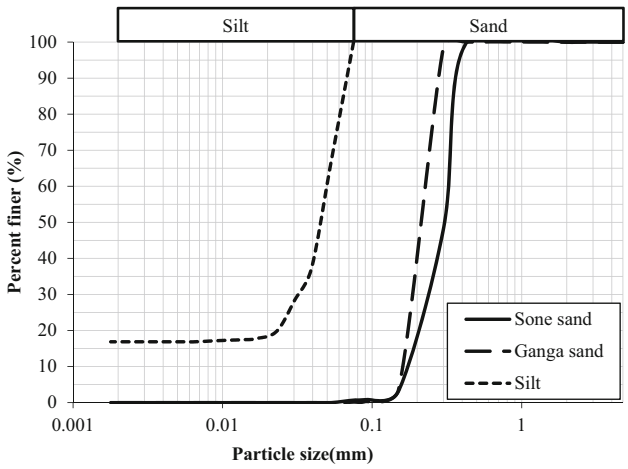

Fig. 1 Particle size distribution curves

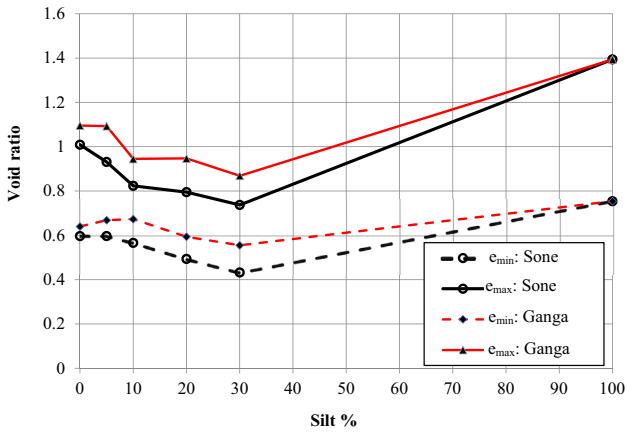

Fig. 2 Maximum (e_{max}) and minimum (e_{min}) void ratio for Sone and Ganga sand at different percentage of silt

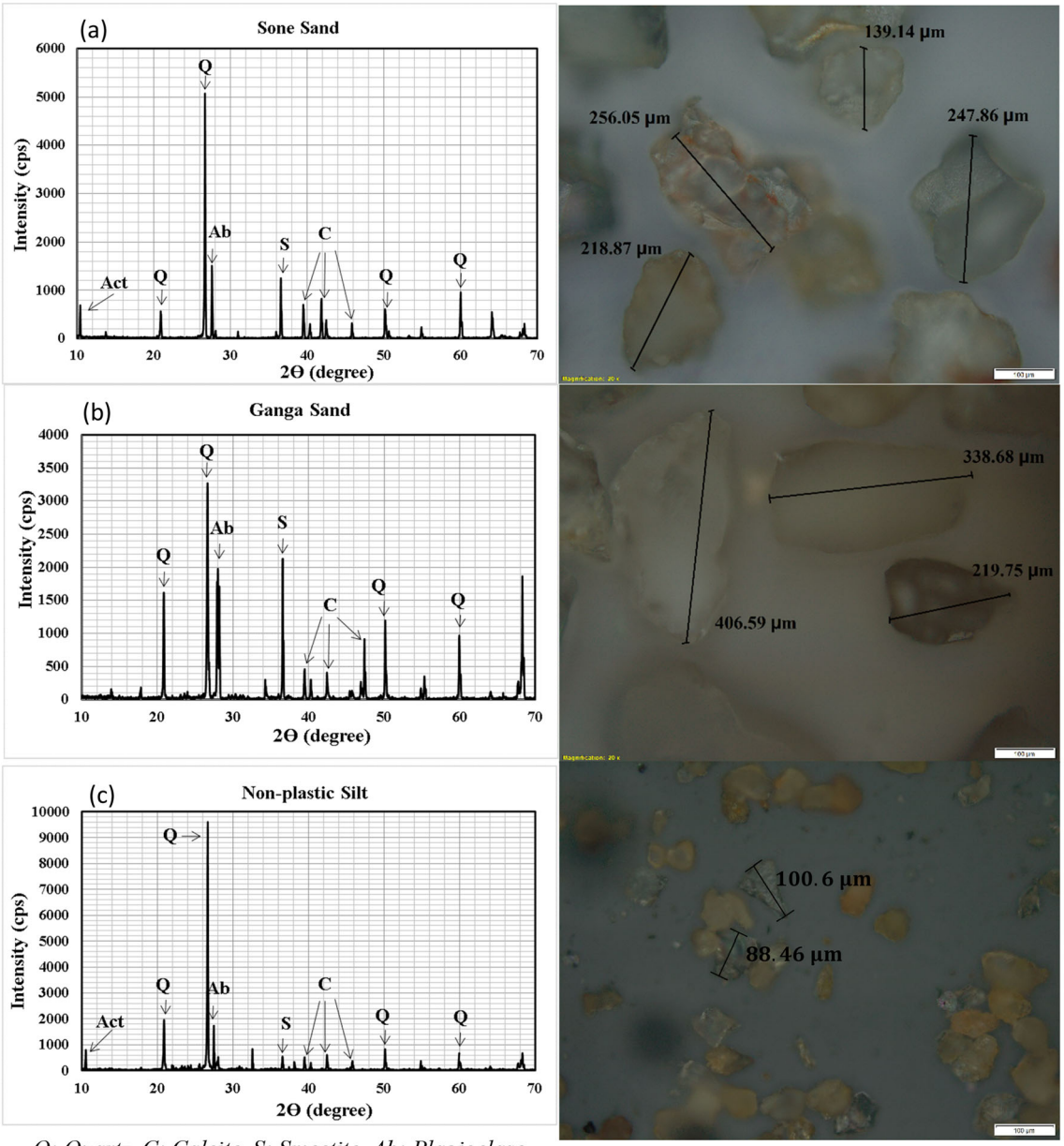

Fig. 3 X-ray diffraction pattern and microscopic view of various soils obtained from the XRD and microscopic analysis (magnification factor = 20) **a** Sone sand, **b** Ganga sand and **c** Silt

was nearly the same for the silty sand prepared using dry pluviation and moist tamping method [36, 37]. Researchers [35, 38] suggested that the specimen prepared using a dry deposition technique replicates the natural deposition of sand. Because of these recommendations and findings, the dry air pluviation method has been adopted in this study as it maintains uniformity in soil specimen. The soil samples were prepared in a split mould of 38 mm diameter and 76 mm height at low relative density (D_r). The soil samples were prepared with an almost similar degree of compactness (Loose, D_r was between 10 and 25%) for each test. The effect of silt intrusion in sandy deposits has been studied in the literature by various approaches (e.g., constant gross void ratio, constant sand skeleton or intergranular void ratio, constant relative density, and limiting fine contents). The seismic behaviour of silty sand has been studied here at a constant relative density of the soil sample. As more and more silts are added to the sand, it passes from the sand dominated matrix to silt dominated matrix. The limiting fines content (LFC) is a threshold value over which further addition of silt in the sand matrix led to loosing of intergranular contacts between sand particles.

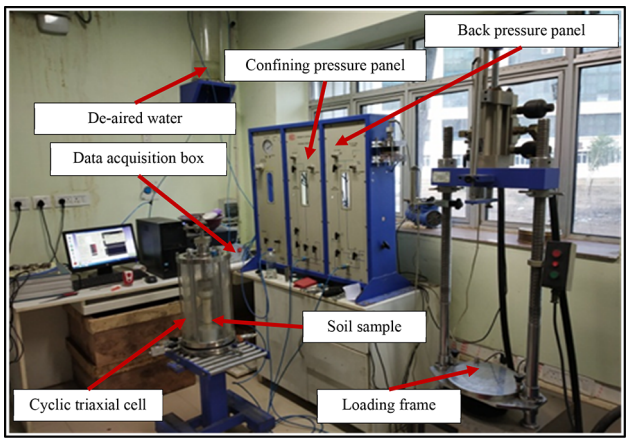

Fig.4 Cyclic triaxial apparatus used in this study

The schematic demonstration of particle arrangement in the sand-silt matrix is shown in Fig. 5. The LFC is very much dependent on particle shape and size and is a unique value for every soil [20]. Using the formula given by [20], the LFC was calculated for both Sone and Ganga river sand and found to be 31 and 29, respectively.

3.2 Sample Saturation and Consolidation

After depositing the soil inside the split mold, the sample cap having a screwed piston rod was placed over it. A suction of 10 kPa was applied to the sample before removing the split mold. Then the cell chamber was attached, which was filled with water to apply the desired (150 kPa) confining pressure. The pressure difference between confining and back pressure value was kept constant (i.e. 20 kPa) during saturation. The degree of saturation was estimated using the Skempton's B parameter after every increment of confining pressure of 20 kPa. Once the desired degree of saturation (greater than 99%) was achieved, the soil specimens were isotropically consolidated to an effecting confining pressure of 150 kPa. At the time of consolidation, the volume change was measured from the volume of water, leaving the system through the back pressure line and getting collected into the volume change indicator device. The soil samples were allowed for consolidation until the volume change has become almost constant. The pre- and post-consolidation relative density of Sone and Ganga sand at different silt percentage are shown in Fig. 6.

3.3 Cyclic Loading

Earthquake loading is highly irregular and is applied to a soil deposit in all three directions. Most of the laboratory cyclic triaxial testing generally apply unidirectional uniform cyclic loadings under stress-controlled or strain-controlled condition. Previous studies claimed that the results obtained from the stress-controlled test consist of unacceptable scattered test data and is very sensitive to sample disturbances, unlike in strain-controlled testing [39]. Cyclic shear strain (γ) is a fundamental parameter governing the cyclic response of sand [40–42]. According to Muley et al. [13] and Vucetic and Dobry [39], excess pore water pressure generation is controlled mainly by the level of induced shear strains. Hence, the present study has been focused on analyzing the behaviour of sand-silt mixture using strain-controlled cyclic triaxial tests. After attaining constant volume change, all the soil specimens were loaded at different cyclic axial strain displacement amplitudes [i.e., ± 0.1 mm (ε = 0.13%), ± 0.5 mm (ε = 0.66%) and ± 1 mm (ε = 1.31%)] with a frequency of 0.5 Hz. The cyclic shear strains corresponding to axial strain levels of 0.13%, 0.66% and 1.31re 0.2%, 0.99% and 1.97% respectively.

4 Test Results and Discussion

4.1 Effect of Soil Type on Liquefaction Strength

The comparison of liquefaction potential of Sone and Ganga sand has been carried out based on the mean grain size diameter ratio ($D_{50\ sand}/D_{50\ silt}$) at the axial strain of 0.66% (± 0.5 mm amplitude). Theoretically, it has been considered that a soil reaches initial liquefaction when the EPWP ratio (r_u) becomes 1, but in practice, it is considered that the soil liquefies before the EPWP value reaches unity [43]. The liquefaction initiation is considered here when EPWP ratio reaches equal to 0.9. Figure 7 presents the liquefaction behaviour of Ganga and Sone sand mixed with various percentages of non-plastic silt. Figure 7a, b present the development of maximum EPWP ratio ($r_{u\ max}$) [44] in

Table 3 Details of cyclic triaxial experiments performed in this study (effective confining pressure = 150 kPa)

Number of tests	Sand type	Silt percentages by weight (%)	Axial displacement amplitude (mm)	Axial strain (%)	Frequency (Hz)
6	Sone river	0, 5, 10, 20, 30, 100	± 0.5	0.66	0.5
6	Ganga river	0, 5, 10, 20, 30, 100	± 0.5	0.66	0.5
3	Sone river	0, 20, 100	± 0.1	0.13	0.5
3	Sone river	0, 20, 100	± 1	1.31	0.5

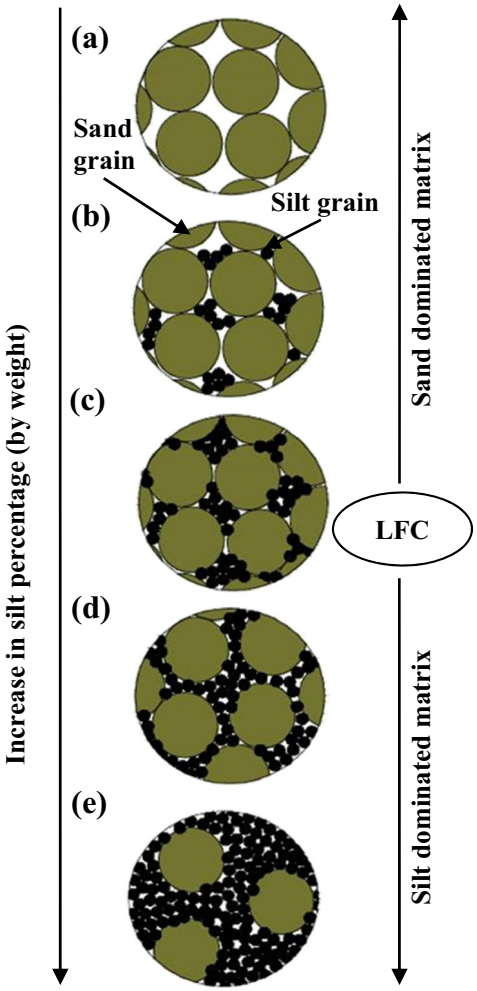

(a) represents the clean sand matrix. It is basically a sand skeleton and hence the void ratio at this stage may also be defined as **sand skeleton void ratio**.

(b) shows that as the silt percentage has been started increasing in clean sand, the voids in sand matrix starts filling with silts

(c) demonstrates a stage at which complete voids of sand matrix get filled by silty particles and the amount of silt at this stage is called as limiting fine content (LFC) or threshold silt content.

(d) and (e) are the particle arrangement after LFC and at this stage, sand particles lose its intergranular contact and starts floating in silt matrix.

Fig. 5 Schematic demonstration of particle arrangement in sand-silt matrix

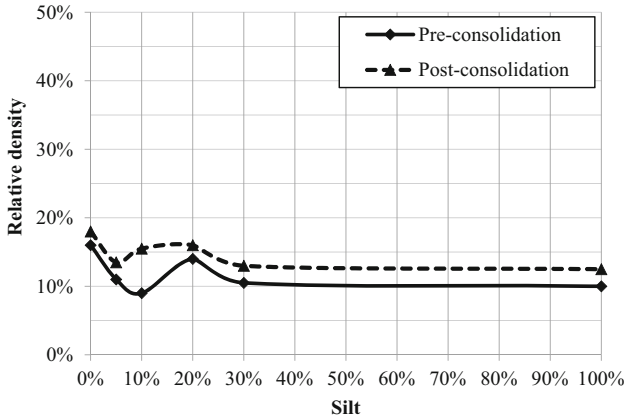

Fig. 6 Pre- and post-consolidation relative density of Sone river sand specimens (at axial strain amplitude of ± 0.5 mm) at different percentages of silt

each cycle of loading. The maximum EPWP signifies the maximum EPWP developed at a particular cycle, as shown in the inset figures. It is quite noticeable that the soil sample with 100% silt has the highest rate of generation of pore water pressure, which is then followed by 30% silt soil sample in both the cases. It is also interesting to note that a lower rate of EPWP development is observed for specimens prepared using 10% silt in both Sone and Ganga river sand. The specimens with 5% and 20% silt content shown more or less similar behaviour in both cases. However, in terms of the overall scenario, it can be ascertained that the rate of development of EPWP was higher in Ganga sand specimens as compared to Sone sand specimens. To demonstrate the behaviour of soil specimen when it liquefies deviatoric stress and axial strain curves has been shown in Fig. 7c, d for Ganga and Sone sand mixed with 20% silt. From the results, it can be inferred that soils have been liquefied with in few cycles.

Alternatively, the same can be ascertained from Fig. 8. Figure 8 delineates the number of cycles at which the soil specimens liquefied. The very first observation is that all

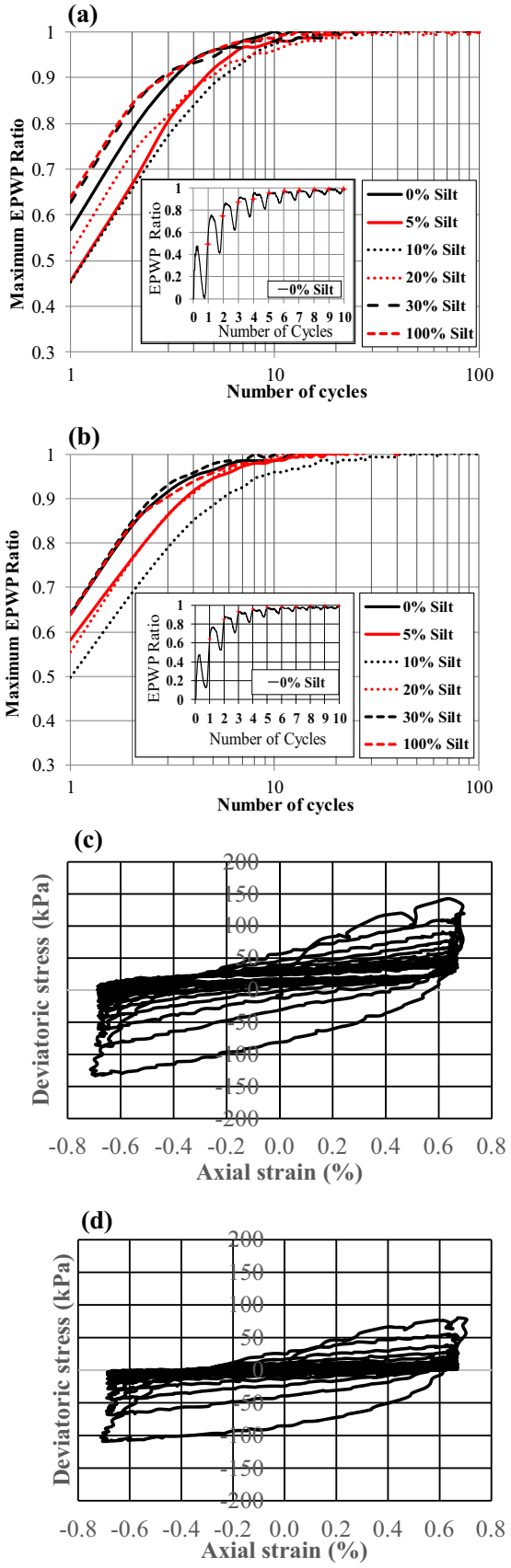

◀**Fig. 7** Maximum EPWP ratio ($r_{u\ max}$) developed at each cycles of loading for axial strain of 0.66% in **a** Sone sand and **b** Ganga sand; deviatoric stress variation with strain for each cycles of loading in **c** Sone sand with 20% silt and **d** Ganga sand with 20% silt

the specimens are getting liquefied within five loading cycles only, and this is because the samples were prepared at low relative density. It can be easily depicted that the number of cycles required for liquefaction occurrence in Ganga sand specimen started decreasing after increasing the silt content beyond 10% silt in the sample. However, the liquefaction resistance remained the same for samples with 5% silt to 20% silt content in Sone sand and beyond that, the liquefaction potential of specimen increased. The similar behaviour has also been observed by [13] on Saloni river sand impinged with different percentages of silt at an axial strain of 0.75%

A couple of previous studies in the literature documented that the soil having a lower $D_{50\ sand}/D_{50\ silt}$ ratio would possess higher liquefaction potential at a lower percentage of silt content [22, 23]. As presented in Table 2, the $D_{50\ sand}/D_{50\ silt}$ ratio was higher for Sone sand. It is evident from Fig. 8 that for every silt-sand mixture, the samples of Ganga sand-silt mixture liquefied earlier than that of Sone sand-silt mixture. As the $D_{50\ sand}/D_{50\ silt}$ ratio of Ganga sand was smaller than Sone sand, due to which the silt particles found it difficult to fit themselves in the intergranular voids of Ganga sand grains. This peculiar characteristic of Ganga sand results in pushing of its grains apart from each other, which in turn reduces the liquefaction resistance at even lower fines content. The results obtained in this study gives very good affirmation to the findings of Monkul and Yamamuro [23] because at the same relative density, same confining pressure and same

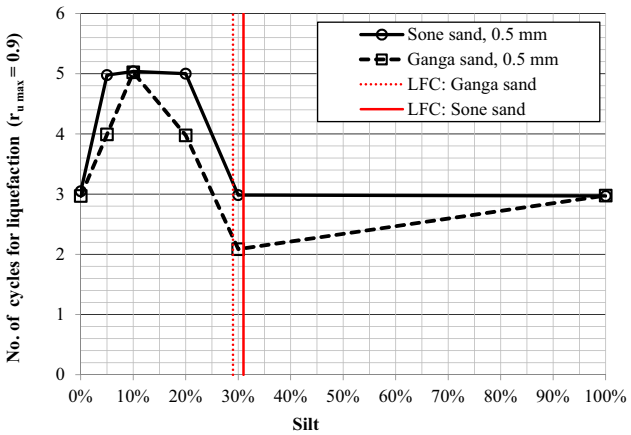

Fig. 8 No. of cycles of loading requisite for liquefaction due to change in silt proportion at axial strain amplitude of ± 0.5 mm

fine content, the liquefaction susceptibility is higher for the soil having less $D_{50\ \mathrm{sand}}/D_{50\ \mathrm{silt}}$ ratio.

4.2 Effect of Silt Percentage on EPWP Model Parameter *F*

As discussed in the previous subsection, the liquefaction strength of studied natural soil depends on the strain amplitude and the silt percentage present in that soil. Dobry et al. [40] proposed a mathematical model for EPWP generation in the soil which was based on the observation from a series of strain-controlled cyclic triaxial tests. The proposed equation is as follow:

$$\frac{1}{r_u} = \frac{1}{p} + \frac{1}{pFfN(\gamma_c - \gamma_{tvc})^s}, \tag{1}$$

where p, F and s are the model parameters, $f = 1$ or 2 depending on whether the loading is one or two-directional, γ_c = cyclic shear strain amplitude and γ_{tvc} = threshold cyclic shear strain amplitude. Based on the literature, it has been observed that the reciprocals of maximum EPWP ratio and the number of cycles followed a linear relationship between them [25]. The Eq. (1) can be represented using the following expression:

$$\frac{1}{r_u} = x\frac{1}{N} + y. \tag{2}$$

In the modified equation, r_u is the maximum EPWP ratio in each loading cycle, and N is the number of loading cycles. The intercept y is almost equal to 1 as the maximum EPWP ratio development in all the cyclic triaxial tests reaches close to unity at the end of the test. So, the parameter p, which is reciprocal of y is also close to 1. However, the slope x is different for different strain amplitudes and effective confining stresses. In the present study, the loading was one-dimensional (1-D), so f was considered as 1, the parameter s also considered as a unity, and the threshold shear strain value was considered as 0.015%.

4.2.1 Variation of the Slope of $1/r_u$ and $1/N$ Plot at Different Silt Content

Figure 9 presents the result of strain-controlled cyclic triaxial tests performed on silt intruded Sone and Ganga sand in terms of $1/N$ and $1/r_u$ for 0.66% axial strain. At a particular shear strain with a y-intercept of $1/p$ an inverse slope of $g(\gamma_c)$. exists in the figure (as shown in Fig. 9), where $g(\gamma_c) = F(\gamma_c - \gamma_{tvc})^s$. The slope has become lowest until the silt content reaches 10% of the total weight of sand in the mixture and increases after that for further increases in the silt content. It is because the silt particles are filling inside the voids of sand skeleton initially. Due to the lower voids, less amount of EPWP has been develop. After a certain percentage (10% in this study) of silt intruded in the sand matrix, sand particles lose contact and start floating in the silt matrix. The variation of the slope with the increase in silt content for various axial train levels has been presented in Fig. 10. It has been observed that this change in the slope due to change in the silt content is less at lower shear strain and more at higher shear strain (shown in Fig. 10). At higher strain, EPWP developed very quickly, which causes a rapid increase in the slope (also observed in [25]).

4.2.2 Variation of EPWP Model Parameter *F* Depending on the Silt Content for Various Sands

The EPWP model parameter F also has been followed a similar trend, as shown in Fig. 11. Tests have been

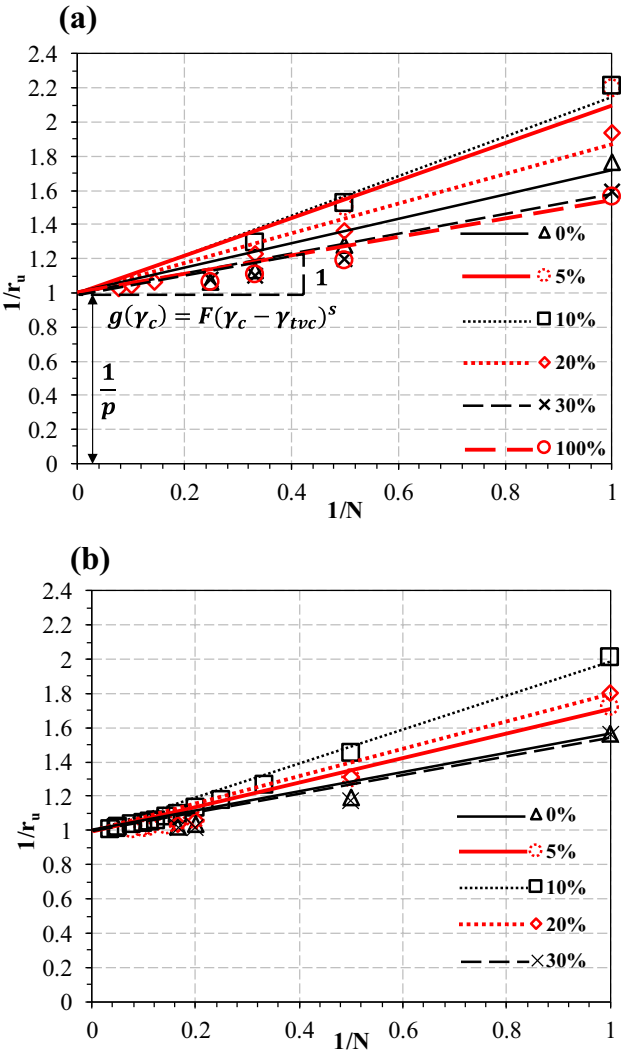

Fig. 9 Relationship between $1/r_u$ and $1/N$ for different percentage of silt intruded (ε = 0.66%) in **a** Sone sand, **b** Ganga sand

performed at intermediate silt contents also at a shear strain level of 0.99% to identify the variation of EPWP model parameter F. It has been observed from results that for 0.99% shear strain, it decreases up to 10% silt content and increases after that. Further, the variation of EPWP model parameter F has been compared for Ganga sand also (as shown in Fig. 12) for an applied shear strain of 0.99%. It can be observed from the figure that for both Ganga and Sone sand, the EPWP model parameter F decreases initially with the increase in the silt content up to 10% and then increases. The possible reason behind it could be the silt dominated soil skeleton formation at higher silt contents in the soil mixture as discussed in Fig. 5 and also by [45].

4.3 Effect of Strain Rate

To evaluate the effect of strain rate on cyclic behaviour of sand-silt mixture, the analysis on Sone sand and non-plastic silt mixed samples has been carried out at two other axial displacement amplitudes also, i.e., at ± 0.1 mm and ± 1 mm. The liquefaction resistance of Sone sand has started decreasing after 20% silt content (as shown in Fig. 8) and which is considered here as threshold silt content. Hence to rationalize, the tests were carried out on three specimens (Sone sand with 0%, 20% and 100% silt contents). Table 4 presents the number of loading cycles at which $r_{u\ max}$ = 0.9 developed at axial displacement amplitudes of 0.1 mm, 0.5 mm and 1 mm. It is evident from the table that soil specimen with 100% non-plastic silt is highly susceptible to liquefaction. However, it has also been observed that at higher axial strain levels (0.66% and 1.31%) the number of cycles required for $r_{u\ max}$ = 0.9 is almost the same for all three specimens.

Jiaer et al. [43] have discussed that shear strain (γ) serves as a very good criterion for seismic performance

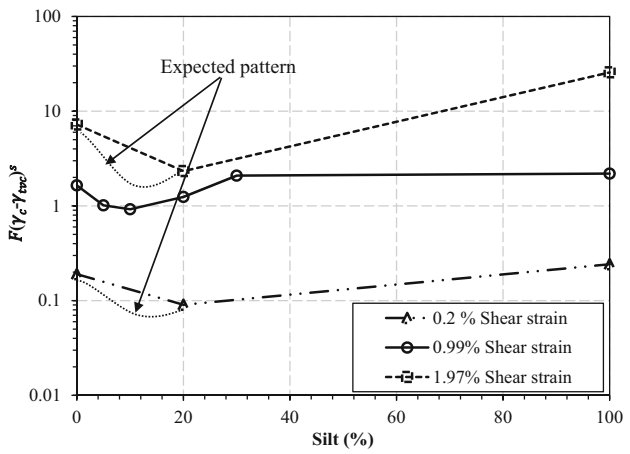

Fig. 10 Variation of the slope of $1/r_u$ and $1/N$ plot with the variation in the silt content at different cyclic shear strain for Sone sand

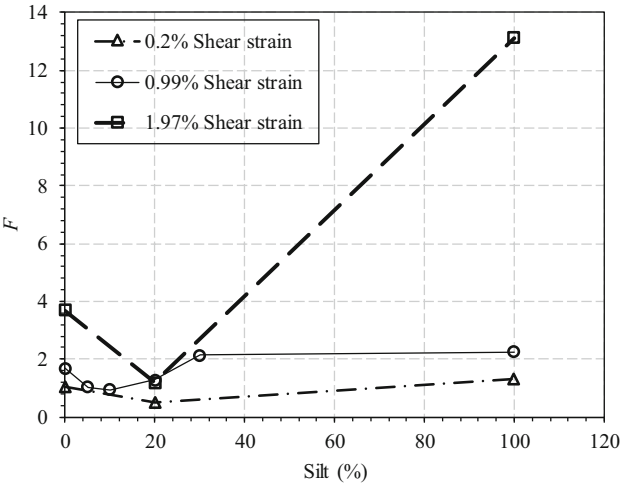

Fig. 11 Variation of the EPWP model parameter F with the variation in silt content at different shear strain for Sone sand

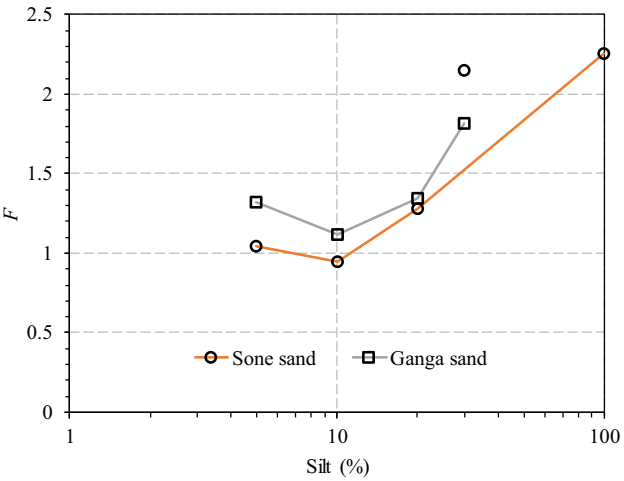

Fig. 12 Variation of the EPWP model parameter F with the variation in the silt content for different sands at large strain (ε = 0.66%)

assessment purposes and the relation between shear and axial strain in undrained triaxial tests is "$\gamma = 1.5 \times \epsilon$". Thus in an attempt to showcase the results in terms of shear strain, Fig. 13 portrays the generation of maximum EPWP ratio in each loading cycle for the soil samples tested at three different shear strains (0.2%, 0.99% and 1.97%). It is quite obvious that a faster rate of EPWP generation has been observed for specimens tested at higher strain amplitudes, and the same can be observed from Fig. 13b, c. Although at higher strains, the $r_{u\ max}$ has become 0.9 within few loading cycles only. However, a contrasting rate of EPWP generation behaviour can be observed for the samples tested at a comparatively lower strain level (shown in Fig. 13a). It is because the soil samples have been prepared at very low relative densities (D_r = 10–25%) due to which they are unable to withstand for longer at higher

Table 4 No. of cycles required for liquefaction at various axial strain levels for Sone sand

Soil specimens	ε = 0.13%	ε = 0.66%	ε = 1.31%
100% sand + 0% silt	100	3	3
80% sand + 20% silt	88	5	2
0% sand + 100% silt	41	3	1

All the values are rounded up to the nearest integer

shear strains. Vis-a-vis the effect of silt can be observed at lower shear strains, i.e., increasing silt content, the liquefaction resistance found to be decreasing.

Hazirbaba and Rathje [46] documented that the rate of generation of EPWP for the sand specimen with 0% and 20% silt content at γ = 0.3% were quite identical which is also having very good agreement to the behavior observed in the present study as shown in Fig. 13a. While little discrepancy observed in the behaviour of sand specimen with 20% silt at γ = 0.2% with the study conducted by Hazirbaba and Rathje [46] can be justified by the presence of more percentage of finer silt particles in the latter case. A higher percentage of fines led to higher pore water pressure development per cycle. As can be observed from the particle size distribution curve shown in Fig. 1 that the particle size of silt used in the present study is ranging from 75 µm to about 20 µm while the silt used in the study conducted by Hazirbaba and Rathje [46] has a minimum particle size of 2 µm.

It is evident that despite varying strain levels, the development of pore water pressure with loading cycles was observed more in the soil specimen having 100% non-plastic silt. Thus it can be easily claimed now that the non-plastic fines are highly susceptible to liquefaction. On comparing clean sand and sand specimen with 20% non-plastic silt, the development of pore water pressure was observed more or less similar at a shear strain of 0.9% and 1.75%. However, a small discrepancy has been observed at a shear strain of 1.75% where the rate of pore water pressure generation is a little bit more than that of clean sand. This anomaly in seismic behaviour of sand can be occurred because, at higher strains, sudden large magnitudes of loads are applied. Sudden load application is more like an application of impact loads, and thus higher pore pressure generation takes place in the soil specimen with less percentage of voids.

5 Conclusion

A series of 18 strain-controlled cyclic triaxial tests were performed using the servo-hydraulic controlled cyclic triaxial testing equipment. The major distinction of this

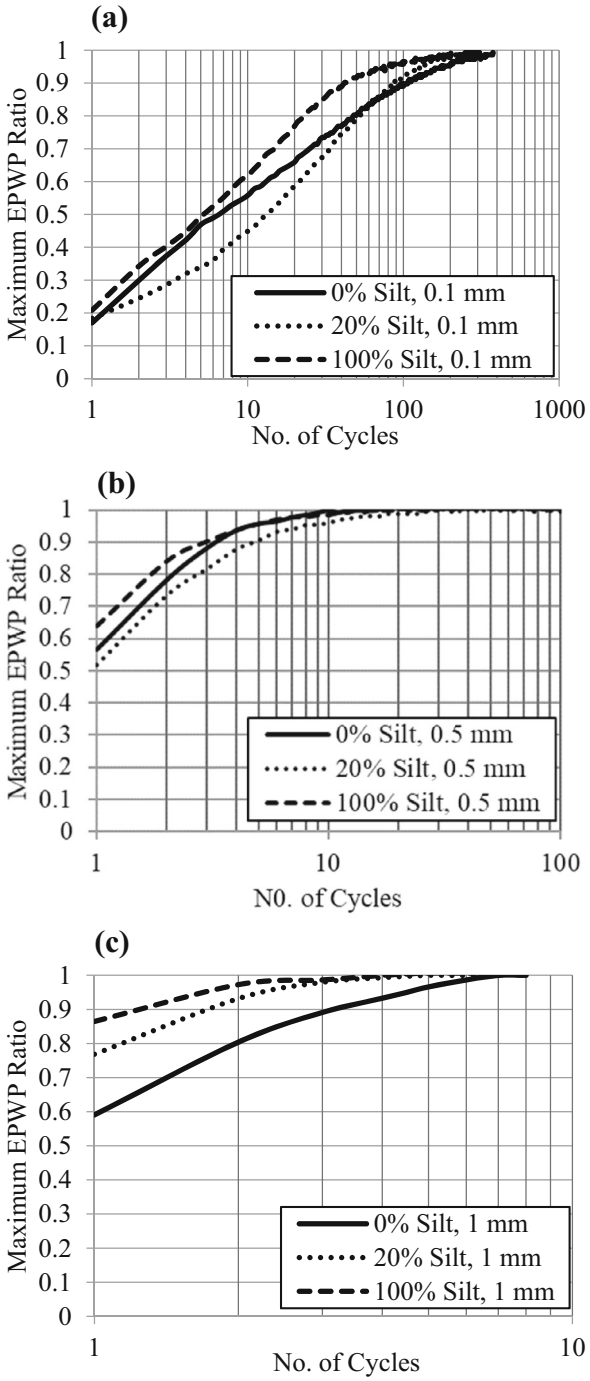

Fig. 13 Maximum EPWP ratio ($r_{u\ max}$) versus number of loading cycles **a** ε = 0.13%, **b** ε = 0.66%, **c** ε = 1. 31%

present study is modifying the EPWP model parameter F for non-plastic silty sands. The EPWP model parameter F has been expressed here as a percentage of silt present in two different sand matrixes. The cyclic behaviour of sand with varying percentage of non-plastic silt has been assessed and explained in terms of mean grain diameter

ratio ($D_{50\ sand}/D_{50\ silt}$). Following conclusion can be drawn from this study:

- Higher rate of excess pore water pressure generation has always been observed for the soil specimen prepared with 100% non-plastic silt at all strain levels. The rate of excess pore water pressure generation was initially found to decrease till 20% and 10% non-plastic silt content in Sone and Ganga sand, respectively. This behaviour was mainly observed because till this time the silt particle could accommodate themselves inside the sand matrix without effecting their intergranular contact.
- Among Sone and Ganga sand, the liquefaction susceptibility of Ganga sand has been found higher than Sone sand at the same relative density, confining pressure, strain level and fines content. Hence, it can be stated that with the increase in $D_{50\ sand}/D_{50\ silt}$ ratio, the liquefaction susceptibility of sand decreases.
- While inspecting the behaviour possessed by Sone river sand at various axial strain levels (i.e., 0.13%, 0.66% and 1.31%), it was found that the effect of non-plastic silt intrusion in the sand could be observed at the lower strain level. The liquefaction resistance of sand decreases with the increase in non-plastic silt proportion at axial strain level of 0.13%. However, at higher axial strain amplitudes (0.66% and 1.31%) the number of cycles required for liquefaction was observed almost the same for the soil specimen with 0%, 20% and 100% non-plastic fines.
- Based on the Dobry's work, EPWP model parameter F has been modified here for various percentages of silt for two different sands (Sone and Ganga river sand). The EPWP model parameter F has been reduced initially (up to 10% silt) as a function of non-plastic silts percentage and increased after that.

It can be inferred from this study that the model parameter F can be modified depending on the percentage of silt particles present in the sand matrix. Further study is required to propose EPWP model parameter F for a wider range of silt percentages.

Acknowledgements The author(s) greatly acknowledge to IIT Patna and Department of Higher Education (Govt. of India) for providing the funding for present research work to carry out the doctoral research study of third author for which no specific Grant number has been allotted.

References

1. Boulanger RW, Idriss IM (2004) Evaluating the potential for liquefaction or cyclic failure of silts and clays. Neurosci Lett 339:123–126
2. Boulanger RW, Idriss IM (2007) Evaluation of cyclic softening in silts and clays. J Geotech Geoenviron Eng 133:641–652. https://doi.org/10.1061/(ASCE)1090-0241(2007)133:6(641)
3. Bray JD, Sancio RB, Riemer MF, Durgunoglu T (2004) Liquefaction susceptibility of fine-grained soils. In: Proceedings of 11th international conference soil dynamics earthquake engineering, 3rd international conference earthquake geotechnical engineering, vol 1. Stallion Press, Singapore, pp 655–62. http://xn–zeta-85a.com.tr/docs/paperno61.pdf. Accessed 12 Sept 2020
4. Taiebat M, Shahir H, Pak A (2007) Study of pore pressure variation during liquefaction using two constitutive models for sand. Soil Dyn Earthq Eng 27:60–72. https://doi.org/10.1016/j.soildyn.2006.03.004
5. Kishida H (1970) Characteristics of liquefaction of level sandy ground during the Tokachioki earthquake. Soils Found 10:103–111. https://doi.org/10.3208/sandf1960.10.2_103
6. Duan W, Cai G, Liu S, Yuan J, Puppala AJ (2019) Assessment of ground improvement by vibro-compaction method for liquefiable deposits from in-situ testing data. Int J Civ Eng 17:723–735. https://doi.org/10.1007/s40999-018-0348-2
7. Andrews DCA, Martin GR (2000) Criteria for liquefaction of silty soils. In: Proceedings of 12th world conference earthquake engineerings, NZ Soc. for EQ Engrg. Upper Hutt, New Zealand. https://www.iitk.ac.in/nicee/wcee/article/0312.pdf. Accessed 12 Sept 2020
8. Thevanayagam S, Fiorillo M, Liang J (2000) Effect of non-plastic fines on undrained cyclic strength of silty sands. Soil Dyn Liq. https://doi.org/10.1061/40520(295)6
9. Xenaki VC, Athanasopoulos GA (2003) Liquefaction resistance of sand–silt mixtures: an experimental investigation of the effect of fines. Soil Dyn Earthq Eng 23:1–12. https://doi.org/10.1016/S0267-7261(02)00210-5
10. Sadrekarimi A (2013) Influence of fines content on liquefied strength of silty sands. Soil Dyn Earthq Eng 55:108–119. https://doi.org/10.1016/j.soildyn.2013.09.008
11. Karim ME, Alam MJ (2014) Effect of non-plastic silt content on the liquefaction behavior of sand–silt mixture. Soil Dyn Earthq Eng 65:142–150. https://doi.org/10.1016/j.soildyn.2014.06.010
12. Hsiao DH, Phan TAV (2014) Effects of silt contents on the static and dynamic properties of sand-silt mixtures. Geomech Eng 7:297–316. https://doi.org/10.12989/gae.2014.7.3.297
13. Muley P, Maheshwari BK, Paul DK (2012) Effect of fines on liquefaction resistance of Solani sand. In: Proceedings of 15th world conference earthquake engineering (Lisbon, Port. Pap. No. 1484, 2012). https://www.iitk.ac.in/nicee/wcee/article/WCEE2012_1484.pdf. Accessed 12 Sept 2020
14. Karim ME, Alam MJ (2017) Effect of nonplastic silt content on undrained shear strength of sand–silt mixtures. Int J Geoeng 8:14. https://doi.org/10.1186/s40703-017-0051-1
15. Nilay N, Chakrabortty P (2021) Evolution in liquefaction strength of Ganga river sand due to intrusion of non-plastic silt. In: Latha Gali M, Raghuveer Rao P (eds) Geohazards. Lecture Notes in Civil Engineering, vol 86. Springer, Singapore. https://doi.org/10.1007/978-981-15-6233-4_19
16. Chang NY, Yeh ST, Kaufman LP (1982) Liquefaction potential of clean and silty sands. In: Proceedings of third international earthquake microzonation conference, Seattle, USA, vol 2, pp 1017–1032
17. Singh S (1996) Liquefaction characteristics of silts. Geotech Geol Eng 14:1–19. https://doi.org/10.1007/BF00431231
18. Amini F, Qi GZ (2000) Liquefaction testing of stratified silty sands. J Geotech Geoenviron Eng 126:208–217. https://doi.org/10.1061/(ASCE)1090-0241(2000)126:3(208)
19. Polito CP, Martin JR II (2001) Effects of nonplastic fines on the liquefaction resistance of sands. J Geotech Geoenvironm Eng

127:408–415. https://doi.org/10.1061/(ASCE)1090-0241(2001)127:5(408)
20. Hazirbaba K (2005) Pore pressure generation characteristics of sands and silty sands: a strain approach. The University of Texas, Austin. https://repositories.lib.utexas.edu/handle/2152/1791. Accessed 12 Sept 2020
21. Dash HK, Sitharam TG (2009) Undrained cyclic pore pressure response of sand–silt mixtures: effect of nonplastic fines and other parameters. Geotech Geol Eng 27:501–517. https://doi.org/10.1007/s10706-009-9252-5
22. Belkhatir M, Arab A, Della N, Missoum H, Schanz T (2010) Influence of inter-granular void ratio on monotonic and cyclic undrained shear response of sandy soils. Comptes Rendus Mec 338:290–303. https://doi.org/10.1016/j.crme.2010.04.002
23. Monkul MM, Yamamuro JA (2011) Influence of silt size and content on liquefaction behavior of sands. Can Geotech J 48:931–942. https://doi.org/10.1139/t11-001
24. Dobry R, Pierce WG, Dyvik R, Thomas GE, Ladd RS (1985) Pore pressure model for cyclic straining of sand. Rensselaer Polytech Institute, Troy
25. Mei X, Olson SM, Hashash YMA (2018) Empirical porewater pressure generation model parameters in 1-D seismic site response analysis. Soil Dyn Earthq Eng 114:563–567. https://doi.org/10.1016/j.soildyn.2018.07.011
26. Chakrabortty P, Roshan AR, Das A (2020) Evaluation of dynamic properties of partially saturated sands using cyclic triaxial tests. Indian Geotech J. https://doi.org/10.1007/s40098-020-00433-3
27. Nilay N (2018) Seismic response of fine saturated sand due to silt intrusion. Indian Institute of Technology Patna
28. IS 2720 (Part 4) (1983) Grain size analysis, Bureau of Indian Standards, Manak Bhawan, 9 Bahadur Shah Zafar Marg, New Delhi, India. https://archive.org/details/gov.in.is.2720.4.1985. Accessed 12 Sept 2020
29. IS 2720 (Part 3) (1980) Determination of specific gravity of soil, Bureau of Indian Standards, Manak Bhawan, 9 Bahadur Shah Zafar Marg, New Delhi, India, (Reaffirmed 2002). https://archive.org/details/gov.in.is.2720.3.2.1980/page/n4. Accessed 12 Sept 2020
30. Lade PV, Liggio CD, Yamamuro JA (1998) Effects of non-plastic fines on minimum and maximum void ratios of sand. Geotech Test J 21:336–347. https://doi.org/10.1520/GTJ11373J
31. IS 2720 (Part 8) (1983) Methods of test for soils: Determination of water content-dry density relation using heavy compaction, Bureau of Indian Standards, Manak Bhawan, 9 Bahadur Shah Zafar Marg, New Delhi, India, (Reaffirmed 2002). https://archive.org/details/gov.in.is.2720.8.1983. Accessed 12th Sept 2020
32. ASTM D4254-16 (2016) Standard test methods for minimum index density and unit weight of soils and calculation of relative density, ASTM International, West Conshohocken, PA. https://doi.org/10.1520/D4254-16
33. IS 2720 (Part 5) (1985) Determination of liquid and plastic limit, Bureau of Indian Standards, Manak Bhawan, 9 Bahadur Shah Zafar Marg, New Delhi, India, (Reaffirmed 2002). https://law.resource.org/pub/in/bis/S03/is.2720.5.1985.pdf. Accessed 12 Sept 2020
34. ASTM D5311-13 (2013) Standard test method for load controlled cyclic triaxial strength of soil, ASTM International, West Conshohocken, PA. https://doi.org/10.1520/D5311_D5311M-13
35. Kuerbis R, Vaid YP (1988) Sand sample preparation-the slurry deposition method. Soils Found 28:107–118. https://doi.org/10.3208/sandf1972.28.4_107
36. Ishihara K (1993) Liquefaction and flow failure during earthquakes. Geotechnique 43:351–451. https://doi.org/10.1680/geot.1993.43.3.351
37. Aziz M, Towhata I, Irfan M (2016) Strength and deformation characteristics of degradable granular soils. Geotech Test J 39:452–461. https://doi.org/10.1520/GTJ20150209
38. Sitharam TG, GovindaRaju L, Srinivasa Murthy BR (2004) Evaluation of liquefaction potential and dynamic properties of silty sand using cyclic triaxial testing. Geotech Test J 27:423–429. https://doi.org/10.1520/GTJ11894
39. Vucetic M, Dobry R (1988) Cyclic triaxial strain-controlled testing of liquefiable sands. Adv. triaxial Test. soil rock, ASTM International. https://doi.org/978-0-8031-5048-5
40. Dobry R, Ladd RS, Yokel FY, Chung RM, Powell D (1982) Prediction of pore water pressure buildup and liquefaction of sands during earthquakes by the cyclic strain method, vol 138. National Bureau of Standards Gaithersburg. https://nehrpsearch.nist.gov/article/PB83-111617/XAB. Accessed 12 Sept 2020
41. Dyvik R, Dobry R, Thomas GE, Pierce WG (1984) Influence of consolidation shear stresses and relative density on threshold strain and pore pressure during cyclic straining of saturated sand. Rensselaer Polytech Institute, Troy, New York. https://erdc-library.erdc.dren.mil/jspui/handle/11681/10255. Accessed 12 Sept 2020
42. Vucetic M (1986) Pore pressure buildup and liquefaction at level sandy sites during earthquakes. Doctoral dissertation, Rensselaer Polytechnic Institute
43. Jiaer WU, Kammerer AM, Riemer MF, Seed RB, Pestana JM (2004) Laboratory study of liquefaction triggering criteria. In: 13th World conference earthquake engineering, Vancouver, BC, Canada. https://www.iitk.ac.in/nicee/wcee/article/13_2580.pdf. Accessed 12 Sept 2020
44. Das A, Chakrabortty P (2020) Influence of motion energy and soil characteristics on seismic ground response of layered soil. Int J Civ Eng 18:763–782. https://doi.org/10.1007/s40999-020-00496-6
45. Thevanayagam S (1998) Effect of fines and confining stress on undrained shear strength of silty sands. J Geotech Geoenviron Eng 124:479–491. https://doi.org/10.1061/(ASCE)1090-0241(1998)124:6(479)
46. Hazirbaba K, Rathje EM (2009) Pore pressure generation of silty sands due to induced cyclic shear strains. J Geotech Geoenviron Eng 135:1892–1905. https://doi.org/10.1061/(ASCE)GT.1943-5606.0000147
47. Erten D, Maher MH (1995) Cyclic undrained behavior of silty sand. Soil Dyn Earthq Eng 14(2):115–123. https://doi.org/10.1016/0267-7261(94)00035-F